Seung-Hyun Kong

High Sensitivity and Fast Acquisition Signal Processing Techniques for GNSS Receivers

From fundamentals to state-of-the-art GNSS acquisition technologies

©ISTOCKPHOTO.COM/COFOTOISME

Higher sensitivity and faster acquisition can be two conflicting goals for a global navigation satellite system (GNSS) acquisition function, and both of the goals must be considered in the development of GNSS signal processing techniques to meet the demands for location-based services (LBSs) in GNSS-challenged environments. This article introduces the fundamentals of GNSS acquisition functions and various GNSS acquisition techniques for new GNSS signals and investigates recent acquisition techniques achieving high sensitivity and fast acquisition. It provides useful information for engineers who study state-of-the-art GNSS signal acquisition techniques and want to understand the challenges involved in improving GNSS acquisition sensitivity and acquisition time.

Introduction

The emergency 911 (E911) phase II requirements issued by the U.S. Federal Communications Commission in 1996 mandated enhanced positioning accuracy of mobile phones and immediate delivery of the positioning results to the public safety answering point (PSAP) [1]. Since then, the global positioning system (GPS) has been both the enabling technology for E911 and rescue services available worldwide and the primary mobile positioning technology for most mobile LBSs.

However, the majority of mobile users are in urban and indoor areas, where GNSS (including GPS) signal propagation is often obstructed by trees, glass, and walls. Consequently, received GNSS signals can be severely attenuated, and it becomes difficult to detect the signals for positioning [2], [3]. In general, the signal attenuation becomes worse when a receiver is deeper indoors. The GPS L1 (frequency) coarse acquisition (C/A) signal has a carrier-to-noise ratio (C/N_0) of about 45 dB-Hz in the outdoor line-of-sight (LOS) environments; however, in the indoor non-LOS (NLOS) environments, the C/N_0 can be far lower than 20 dB-Hz [2], [3]. Therefore, GNSS signal acquisition in GNSS-challenged environments (such as urban and indoor) requires very high sensitivity, for which a huge increase of both acquisition complexity (i.e., computational cost and hardware usage) and acquisition time

Digital Object Identifier 10.1109/MSP.2017.2714201
Date of publication: 6 September 2017

is unavoidable. As a result, a high sensitivity and fast acquisition technique is necessary for GNSS receivers operating in GNSS-challenged environments.

This article covers a broad range of technical topics in GNSS acquisition for standalone and assisted GNSS receivers. The first half of this article introduces the fundamentals of conventional GNSS acquisition techniques and the acquisition techniques for new GNSS signals with various modulation schemes, while the second half focuses on the recent signal processing techniques for GNSS acquisition that achieve high sensitivity and fast acquisition with low computational cost by utilizing specialized signal processing algorithms and search strategies different from the conventional acquisition techniques.

Fundamentals of GNSS signal acquisition

The GNSS signal acquisition function in a GNSS receiver searches and detects incoming GNSS signals to initialize the tracking function that actually produces fine GNSS signal measurements for positioning. In general, the GNSS signals are spread by periodic long spreading codes, and the GNSS satellite motion relative to the receiver generates a Doppler-frequency shift in the incoming signal as large as 5–10 kHz depending on the receiver's motion. Since the precise time and location of a GNSS receiver is initially unknown, the goal of the GNSS acquisition function is to identify the prompt code phases and Doppler frequencies of the incoming GNSS signals as quickly as possible, within a resolution fine enough to initialize the tracking function successfully. Because the code phase and Doppler frequency of an incoming GNSS signal can be at any hypothesis on the two-dimensional (2-D) hypothesis plane (also known as the *search space*), the acquisition function may need to test every hypothesis within the search space using a matched filter (e.g., correlator) [2]–[4] to detect the incoming GNSS signal.

In general, the acquisition process can be both time consuming and computationally expensive when a GNSS receiver tries to acquire weak GNSS signals (see the section "GNSS Signal Model and Integration Techniques"). Conventionally, the number of code-phase hypotheses N_{Hc} for binary phase-shift keying (BPSK)-modulated GNSS signals is set to two times the spreading code length L_c (in other words, the code-phase search step size Δ_τ is set to a half code chip). On the other hand, the number of Doppler-frequency hypotheses N_{Hf} can grow when the user dynamics relative to the satellite motion is large and the Doppler-frequency search step size Δ_f is small, where Δ_f is inversely proportional to the coherent correlation interval T_{co} [2]–[4] (see the section "Search Strategy for Lower Acquisition Complexity"). In fact, to detect a weaker GNSS signal, longer T_{co} is necessary, and the number of Doppler-frequency hypotheses increases consequently. As a result, both the acquisition time and acquisition complexity for weaker GNSS signals increase exponentially due to the longer time to test each hypothesis and the larger number of hypotheses in the search space. Note that the increase of acquisition complexity is not a critical problem for GNSS receivers in open-sky outdoor environments, where the signal attenuation can be negligible.

To lessen the acquisition time and complexity, a GNSS receiver needs to select an appropriate integration technique, search strategy, and detection scheme based on the GNSS signal modulation, signal strength, available hardware resources, computational capacity of the receiver, and target mean acquisition time (MAT), i.e., the expected time for signal acquisition, etc. Next we introduce the conventional integration techniques, search strategies, and detection schemes that involve the detection variables and detection thresholds.

GNSS signal model and integration techniques

A hypothesis testing utilizes the autocorrelation function (ACF) [2]–[4] that performs correlation between the incoming GNSS signal $y(t)$ that is downconverted to an intermediate frequency (IF) f_I and a receiver replica signal $x(t)$. In GNSSs, various signal modulation schemes are used for satellite signals in multiple frequencies. The conventional GPS civil signal (i.e., L1 C/A signal) and Glonass L1 C/A signal use BPSK modulation, and most new GNSS signals employ modulation schemes to separate the data and pilot channels and additional binary offset carrier (BOC) modulation to separate the mainlobe of the signal spectrum into lower and upper mainlobes to the carrier frequency. Currently, there are more than eight variants of BOC modulations used or being planned for the new GNSS signals [5]. Therefore, there should be a number of mathematical expressions required for $y(t)$. However, in this article, we consider three conventional modulation schemes of $y(t)$ commonly used for GNSS acquisition functions, as shown in the box at the bottom of the page, where the subscripts D and P denote data and pilot channels, respectively; A represents the amplitude; $D(t)$ is the binary phase-modulated navigation data at a data rate $R_b(=1/T_b)$; $P(t)$ and $S(t)$ are the binary phase-modulated primary and secondary spreading codes, respectively; $SC(t)$ denotes the subcarrier signal; τ, f_D, and θ are the unknown delay, Doppler frequency, and phase of the incoming signal, respectively; and $v(t)$ represents the complex additive white Gaussian noise process with two-sided power spectral density $N_0/2$. In addition, the length and the chip rate of $P(t)$ are denoted as L_c and $R_c(=1/T_c)$, respectively. Note that (1a) includes GPS

$$y(t)=\begin{cases} AD(t-\tau)P(t-\tau)\cos(2\pi(f_I+f_D)t+\theta)+v(t), & \text{for BPSK} \quad (1a)\\ A_D D(t-\tau)P_D(t-\tau)S_D(t-\tau)SC_D(t-\tau)\cos(2\pi(f_I+f_D)t+\theta) & \\ \quad +A_P P_P(t-\tau)S_P(t-\tau)SC_P(t-\tau)\sin(2\pi(f_I+f_D)t+\theta)+v(t), & \text{for QPSK} \quad (1b)\\ \left[A_D D(t-\tau)P_D(t-\tau)SC_D(t-\tau)+A_P P_P(t-\tau)SC_P(t-\tau)\right] & \\ \quad \times\cos(2\pi(f_I+f_D)t+\theta)+v(t), & \text{for in phase,} \quad (1c) \end{cases}$$

Table 1. Channel parameters of some GNSS signals that belong to (1a)–(1c).

	A_P/A_D	$D(t)$	$P_P(t)$	$P_D(t)$	$S_P(t)$	$S_D(t)$	$SC_P(t)$	$SC_D(t)$	
GPS L1 C/A	–	$R_b = 50$	–	$L_c = 1023$ $R_c = 1.023$	–	–	–	–	(1a)
GPS L2C	CM and CL codes are chip-by-chip multiplexed	$R_s = 50$	$L_c = 767,250$ $R_c = 0.5115$	$L_c = 10230$ $R_c = 0.5115$	–	–	–	–	(1c)
GPS L5	1	$R_s = 50$	$L_c = 10230$ $R_c = 10.23$	$L_c = 10230$ $R_c = 10.23$	$L_c = 20$ $R_c = 0.001$	$L_c = 10$ $R_c = 0.001$	–	–	(1b)
Galileo E1 OS	1	$R_s = 250$	$L_c = 4092$ $R_c = 1.023$	$L_c = 4092$ $R_c = 10.23$	$L_c = 25$ $R_c = 250$ Hz	–	CBOC(–)	CBOC(+)	(1c)
Galileo E5a	1	$R_s = 50$	$L_c = 10230$ $R_c = 10.23$	$L_c = 10230$ $R_c = 10.23$	$L_c = 100$ $R_c = 0.001$	$L_c = 20$ $R_c = 0.001$	–	–	(1b)
Glonass L1 C/A	–	$R_s = 50$	–	$L_c 511$ $R_c = 0.511$	–	–	–	–	(1a)

Note that CBOC(±) = $\sqrt{10/11}$ sinBOC(1, 1) ± $\sqrt{1/11}$ sinBOC(1, 1), where sinBOC(1,1)= sign[sin(2 $\pi R_c t$)].

L1 C/A and Glonass L1 C/A signals and (1b) can be used for GPS L5, Galileo E5a, and Galileo E5b signals, where pilot and data channels are modulated by quadrature phase-shift keying (QPSK); and (1c) is for GPS L1C, GPS L2C, Galileo E1 OS (open service), and (maybe) BeiDou B1, where signals are separated by the spreading code or by time-division multiplexing. Note that the BeiDou B1 modulation scheme is not fixed yet at the time of writing this article, but it is found in [5] that one of the most probable options for BeiDou B1 is a combination of a BPSK-modulated data channel and a quadrature-multiplexed BOC (QMBOC)-modulated pilot channel, where, in QMBOC, the pilot channel has most (88%) of its power in the same phase and the rest in the quadrature phase to the data channel. Therefore, an acquisition function may process the BeiDou B1 signal as an in-phase signal in (1c) to reduce the receiver complexity. Note also that Galileo E5 alternate BOC (AltBOC) modulation cannot be expressed using (1b); however, the lower and upper mainlobes of Galileo E5 AltBOC can be represented by two QPSK-modulated signals in (1b), respectively. The channel parameters of some of the GNSS signals belonging to (1a), (1b), and (1c) are summarized in Table 1 [5], where the unspecified units of R_b, R_s (encoded symbol rate), L_c, and R_c are bits/s, symbols/s, chips, and megahertz (MHz), respectively.

The acquisition functions for the GNSS signals in (1b) and (1c) are discussed in the section "Channel Combining Techniques for New GNSS Signals." In this section, we use the GPS L1 C/A signal (1a) to introduce the fundamentals of GNSS acquisition and let T_p, T_1, and T_{20} represent the primary code period in seconds, 1 ms, and 20 ms, respectively. To detect the prompt code phase τ and Doppler frequency f_D of an incoming GNSS signal, an acquisition function performs a correlation at the time instant η between the incoming signal $y(t)$ and a receiver replica $x(t)$ for the κth code phase and λth Doppler-frequency hypothesis (in a complex form)

$$x(t;\kappa,\lambda) = P(t-\kappa\Delta_\tau)e^{j2\pi(f_I+\lambda\Delta_f)t} \tag{2}$$

to generate a correlation output for the κth code phase and λth Doppler-frequency hypothesis as

$$R[\eta,\kappa,\lambda] = \sum_{n=0}^{N_{co}-1} y[n+\eta]x[n;\kappa,\lambda], \tag{3}$$

where N_{co} is the number of samples received during the coherent correlation interval T_{co} for a sampling frequency f_s (i.e., $N_{co} = f_s T_{co}$) and $R[\eta,\kappa,\lambda] = R^I[\eta,\kappa,\lambda] + jR^Q[\eta,\kappa,\lambda]$. In general, the acquisition function employs a (postcorrelation) integration function $G(\cdot)$, as shown in Figure 1, that combines the pilot and data channel components and integrates consecutive correlation outputs to further increase the acquisition sensitivity. The integration techniques for $G(\cdot)$ are introduced using the GPS L1 C/A signal as an example, and the channel-combining techniques are introduced in the section "Channel Combining Techniques for New GNSS Signals."

Coherent integration technique

When the coherent correlation interval T_{co} is much smaller than T_b as in the conventional GPS L1 C/A signal receivers that use $T_{co} = T_1 = 1$ ms, the data $D(t)$ can be assumed constant during an integration. Therefore, the resulting consecutive coherent correlation outputs can be coherently added for N_i $(1 \le N_i < 20)$ times to build a coherently integrated detection variable $Z = Z_{co}$, as in Table 2. Note that N_i is called the *accumulation length*, and that Z_{co} is equivalent to the detection variable for a coherent correlation with a long coherent correlation interval $N_i T_{co}$. In general, this technique amplifies the signal peak amplitude (i.e., $\sqrt{Z_{co} \mid H_1}$) by N_i times. However, when $N_i \gg 1$, there can be bit transition(s) during the overall interval $N_i T_{co}$, which often causes a significant degradation of the signal peak power, $Z_{co} \mid H_1$.

Noncoherent integration technique

To avoid the bit transition problem in the long coherent integration, an acquisition function may choose T_{co} much smaller than

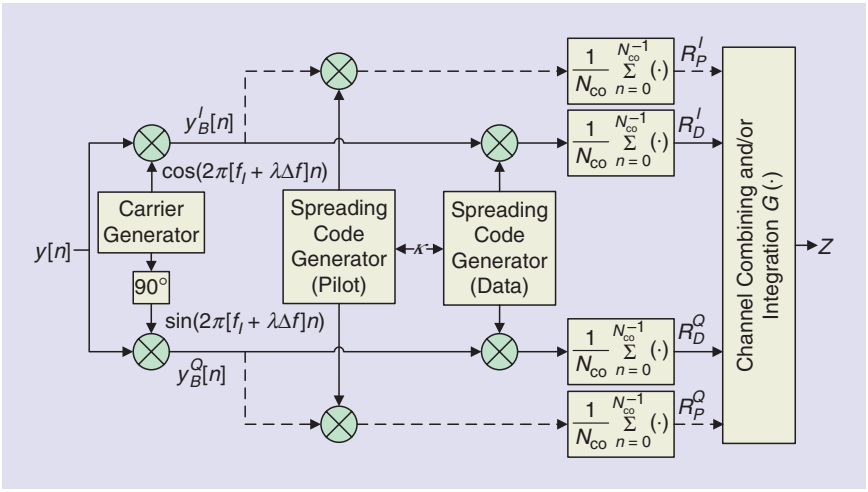

FIGURE 1. A diagram for the correlation, combining, and integration function to test a hypothesis at $[\kappa, \lambda]$. The dotted lines are for the pilot channel, the solid lines are for the data channel, and the superscripts I and Q represent the in-phase and quadrature-phase components, respectively.

Table 2. Detection variables of various integration techniques.

Integration Techniques	Detection Variable for the κth Code Phase and λth Doppler-Frequency Hypothesis
Coherent	$Z_{co}[\kappa,\lambda] = \left\lvert \sum_{\eta=0}^{N_i-1} R[\eta,\kappa,\lambda] \right\rvert^2$
Noncoherent	$Z_{nc}[\kappa,\lambda] = \sum_{\eta=0}^{N_i-1} \lvert R[\eta,\kappa,\lambda] \rvert^2$
Differentially coherent	$Z_{di}^1[\kappa,\lambda] = \left\lvert \sum_{\eta=1}^{N_i-1} R[\eta,\kappa,\lambda] \times R^*[\eta-1,\kappa,\lambda] \right\rvert^2$
MGDC	$Z_{mgdc}[\kappa,\lambda] = \sum_{m=1}^{N_i-1} \lvert Z_{di}^m[\kappa,\lambda] \rvert = \sum_{m=1}^{N_i-1} \left\lvert \sum_{\eta=m}^{N_i-1} R[\eta,\kappa,\lambda] \times R^*[\eta-m,\kappa,\lambda] \right\rvert$

T_b and noncoherently combines N_i consecutive coherent correlation outputs by taking the sum of squares of each coherent correlation output to build a detection variable Z_{nc}. As a result, Z_{nc} is immune to both the bit transition problem and the phase shift in the consecutive correlation outputs. However, the resulting increase in the signal peak amplitude after the N_i times noncoherent accumulation is much less than N_i times, and the technique suffers from the squaring loss [3] for weak GNSS signals.

Differential integration technique

Another possible scheme to cope with the bit transition problem is to multiply the prompt (at time instant η) coherent correlation output with the conjugate of the previous one (at time instant η-1) and coherently accumulate the consecutive results to build a differential coherently integrated detection variable Z_{di}^1 [6], where the superscript 1 represents the one span. This technique exploits the fact that the signal components in consecutive correlation outputs (e.g., $R[\eta_1,\tau,\lambda]$ and $R[\eta_2,\tau,\lambda]$) that are separated by a unit correlation interval (i.e., $\eta_2-\eta_1 = 1$ span) have the same (or similar) phase, while the noise components are independent. However, there can be a monotonous phase shift between the consecutive correlation outputs, which can result in a signal-to-noise ratio (SNR) loss in Z_{di}^1. To cope with the phase shift, the modified general differential combination (MGDC) technique [7] uses Z_{mgdc} that noncoherently accumulates the differential coherently integrated detection variables of all possible spans (from 1 to N_i-1 span). The MGDC shows a higher robustness against the phase shift than the general difference combination (GDC) technique [8], which coherently accumulates the differential coherently integrated detection variables of all possible spans. The MGDC technique is useful for combining partial correlation outputs of GNSS signals that have long spreading codes, such as GPS L2C, without degrading the performance due to the bit transitions [9]. The SNR improvement with Z_{mgdc} is higher than Z_{nc} but much lower than Z_{co} because of the noise amplification caused by the multiplication of noise components in the two multiplied correlation outputs.

Note that the detection variables in the aforementioned integration techniques are different and have different statistical distributions (in the presence and absence of the signal), and, as a result, each of these integration techniques has different probabilities of detection (P_d), misdetection (P_m), and false alarm (P_f) in the individual hypothesis tests. Also, note that the detection variables in Table 2 have magnitude-squared function but can also have different nonlinear function [3].

Search strategy for lower acquisition complexity

In general, the code-phase search step size Δ_τ is set to a half-chip ($T_c/2$) for BPSK signals (1a) so that the total number of code-phase hypotheses N_{Hc} is two times the code length L_c. On the other hand, the total number of Doppler-frequency hypotheses N_{Hf} is $2\lceil f_{max}^D/\Delta_f \rceil + 1$, since the Doppler-frequency search is from the negative to positive maximum Doppler frequencies, i.e., $-f_{max}^D$ to $+f_{max}^D$, with a step size Δ_f, where $\lceil(\cdot)\rceil$ is the ceiling operator. Since $\Delta_f = 1/(2T_{co})$ [3] and $f_{max}^D = 5$ kHz (or more) are one of the common choices, the maximum number of hypothesis to test is $N_H = 2L_c \times (2\lceil f_{max}^D/\Delta_f \rceil + 1) \cong 4L_c\lceil 2f_{max}^D T_{co} \rceil$. Note that $\Delta_f = 2/(3T_{co})$ can be used [2], f_{max}^D=10 kHz is possible for dynamic receivers, and the choice of $\Delta_f > 1/(2T_{co})$ causes larger SNR loss in the correlation output but smaller N_H than the choice of $\Delta_f = 1/(2T_{co})$, for example, $\Delta_f = 2/(3T_{co})$ may cause 1 dB lower SNR than $\Delta_f = 1/(2T_{co})$. For an example with a simple GPS L1 C/A signal acquisition function using a single correlator with $T_{co} = 1$ ms and $N_i = 1$, each of the

N_H ($\cong 41{,}000$) hypotheses is tested serially (which is why it is called the *serial search*), and, assuming the true (correct) hypothesis H_1 can be any one of the N_H hypotheses, the mean and worst-case acquisition times can be $(1/2)N_H T_{\text{co}} = 20.5$ s and $N_H T_{\text{co}} = 41$ s, respectively. The MAT (μ_T) can grow exponentially for acquisition functions using the serial search strategy when, for example, N_i times longer coherent integration length is used; N_i times longer time to test each hypothesis and N_i times larger number of Doppler-frequency hypotheses result in MAT increased by N_i^2 times. Therefore, it is necessary to have an effective search strategy to reduce the MAT for the given hardware and computational capacities to a GNSS receiver.

Multiple-dwell search strategy

To reduce the MAT μ_T, a receiver with a single correlator may employ the double- (or multiple-) dwell search strategy [10]. The idea is to test hypothesis using a shorter correlation time (also known as *dwell time*) in the first stage of search to quickly distinguish the true hypotheses H_1 from the incorrect hypotheses (H_0's). As an example, in the first stage of a double-dwell search strategy, an acquisition function performs hypothesis testing with a smaller coherent dwell time $T_{\text{co},1}$, and when a correlation output is found larger than the first stage threshold γ_1, the acquisition function performs the second test for the same hypothesis using a longer coherent dwell time $T_{\text{co},2} (> T_{\text{co},1})$ and a larger threshold $\gamma_2 (> \gamma_1)$. As a result, the MAT of the double-dwell search, $\mu_{T,D}$, can be roughly one half of $\mu_{T,S}$ for $T_{\text{co},1} = T_{\text{co}}/2$ when the incoming signal is strong enough (i.e., when P_m and P_f are negligible), where the subscripts S and D represent the single and double-dwell searches, respectively. In general, in the multiple-dwell search, longer dwell time and higher detection threshold are used in the latter stages, and the detection threshold for each stage needs to be carefully selected for optimal acquisition performance, i.e., the minimum MAT.

Parallel (complete) search strategy

In the parallel (or complete) search strategy, a GNSS receiver tests all of the hypotheses in the search space and identifies the true hypothesis H_1 from the complete search result. Testing all of the hypotheses in parallel may require a massive amount of correlators, so this search strategy requires the highest acquisition complexity. Conventionally, the maximum integration output of the complete search result, $\max\{Z\}$, is used as the detection variable to be compared to the detection threshold, which is similar to the hybrid search strategy in the following. In practice, when using the parallel and hybrid search strategies, there are options for the detection variables and detection schemes, as discussed in the section "Detection Schemes."

Hybrid search strategy

In the hybrid search strategy, a subset of all hypotheses is tested simultaneously at a time. As an example, a receiver utilizes N_{Hc} (or N_{Hf}) correlators in parallel to test the N_{Hc} code-phase hypotheses for each Doppler-frequency hypothesis (or vice versa) at the same time. Figure 2 depicts a time-domain acquisition function employing a hybrid search strategy with M parallel correlators, where D represents a half-chip delay. The acquisition function in Figure 2 can achieve about M times smaller MAT than $\mu_{T,S}$ when the incoming signal is strong enough and can be realized in the frequency domain, as shown in Figure 3. The incoming signal samples $y[n]$ and receiver replica $x[n]$ are collected for one code period (T_p) to build y and x vectors of the same size $N_{\text{co}} (= f_s T_p)$, respectively, and it is found that

$$\text{rev}[x] \circledast y = \text{IDFT}\{\text{DFT}\{x\}^* \cdot \text{DFT}\{y\}\} = \text{IDFT}\{X^* \cdot Y\}, \tag{4}$$

where $\circledast$ is the circular convolution operator; $\text{rev}[x] = \{x[n] \mid n = N_{\text{co}}, N_{\text{co}} - 1, \ldots, 1\}$; $\text{DFT}\{\cdot\}$ and $\text{IDFT}\{\cdot\}$ are the discrete Fourier transform and inverse DFT operations, respectively; the superscript * represents the complex conjugate operation; $X = \text{DFT}\{x\}$; and $Y = \text{DFT}\{y\}$. Each $\text{IDFT}\{X^* \cdot Y\}$ result in (4) is used for the signal detection, and similarly to the parallel search strategy there are options of detection variables and detection schemes used for the hybrid search strategy in practice. The frequency-domain hybrid search can be implemented with a digital signal processor (DSP) chip, so it should be useful to reduce both computational cost and MAT

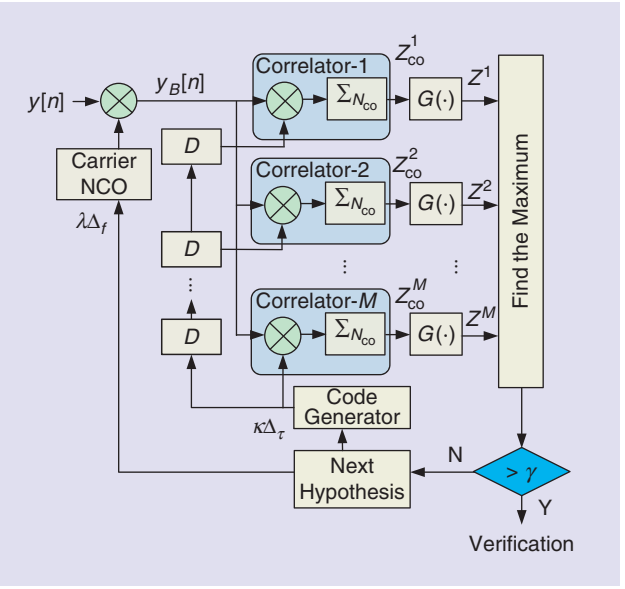

FIGURE 2. The time-domain parallel/hybrid search with MTC.

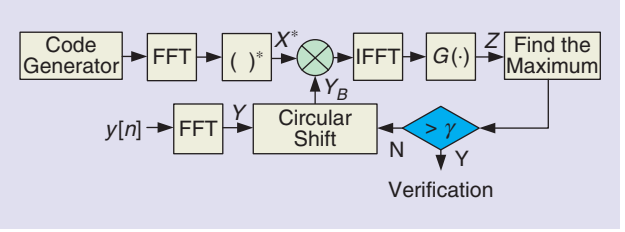

FIGURE 3. The frequency-domain parallel/hybrid search with MTC.

for weaker GNSS signal acquisition. In the literature, the mean acquisition computation (MAC) (μ_C, i.e., the expected computational cost for a signal acquisition) is used for a measure of the mean computational cost of acquisition [11]. Note that, in practice, X^* can be pregenerated and stored in a memory of a receiver, and fast Fourier transform (FFT) and inverse FFT (IFFT) are used instead of DFT and IDFT, respectively, which effectively reduces the computational cost. Figure 3 shows the FFT-based hybrid search technique (FFT-based technique, for short), where, due to the circular convolution in the FFT-based correlation [12], x is padded with N_{co} (or more) zeros to make the length of X equal to an integer power of two, and y of the same size should be used to obtain Y. The circular shifting of Y in Figure 3 is to shift the Doppler-frequency hypothesis to the next one. As a result, the overall amount of complex multiplications for the FFT-based technique has an order of $\mathrm{O}(N_{\text{co}} \log 2N_{\text{co}})$.

Note that, while an acquisition function can employ the serial, parallel, or hybrid search strategy depending on the available receiver capacity, the multiple-dwell search can be used in combination to the search strategy to speed up the acquisition. When the detection variable is found to be larger than the threshold, the verification function additionally tests the detected hypothesis multiple times to verify the acquisition. Since the detected code phase and Doppler frequency by the acquisition function have errors as large as $\Delta_\tau/2$ and $\Delta_f/2$, respectively, the pull-in search process is employed to find a finer-Doppler-frequency estimate, and then the signal tracking function estimates and tracks the precise code phase and Doppler frequency of the incoming signal to produce measurements for positioning.

Detection schemes

In GNSSs, a detection scheme involves a detection variable and a detection rule for reliable signal detection from the search result. In practice, the selection of the detection variable may depend on the employed search strategy as discussed next.

Threshold crossing

In the serial search, the integration function $G(\cdot)$ output resulting from the current hypothesis test is used as the detection variable, and a detection is declared when the detection variable is found to be larger than the detection threshold γ. This detection rule is called the *threshold crossing* (*TC*) [10] and is used only for the serial search strategy. The overall system performance of the acquisition function using TC can be expressed with the system probabilities [13]: the detection P_D, misdetection P_M, and false alarm P_F probabilities. Note that the system probabilities are different from those (P_d, P_m, and P_f) of the individual hypothesis test, since the system probabilities represent the performance of the overall acquisition function, while P_d, P_m, and P_f are related to the detection performance of each individual hypothesis test.

Maximum TC and maximum-to-second-maximum ratio

For acquisition functions employing the hybrid or parallel search strategy, the maximum of the integration function $G(\cdot)$ output (in other words, the maximum of the current search result) is often used as the detection variable and is compared to the detection threshold, which is the maximum TC (MTC) scheme [14] shown in Figures 2 and 3. Note that, in the hybrid search strategy, the maximum of the integration function output is only a local maximum. In practice, the maximum-to-second-maximum ratio [15] (MTSMR) of the search result can be used as the detection variable, where the second maximum should be at least one chip apart from the maximum. In [16], the system probabilities, i.e., P_D, P_M, and P_F, of the acquisition function using MTC are very similar to those using MTSMR.

K-largest

The *K*-largest detection rule has been used successfully in practice [17], where an acquisition function selects $K(>1)$ hypotheses that produce the *K*-largest integration function outputs. To verify the detection, a receiver tests the selected K hypotheses again to identify the true hypothesis. This detection rule can be used for both hybrid and parallel search strategies and has been found useful for detecting the GNSS signal in noise, since the probability that the true hypothesis H_1 is included within the *K*-largest hypotheses is higher than the probability that H_1 is at the maximum of the integration function output.

Detection threshold

The detection threshold γ has a critical effect on the acquisition performance, since it affects both the probabilities (i.e., P_d, P_m, and P_f) of the individual hypothesis testing and the system probabilities (i.e., P_D, P_M, and P_F,) of the acquisition function. The conventional technique for determining the detection threshold is to find a γ that limits P_f under a tolerable small constant level (e.g., 0.01 or less), known as the *constant false alarm rate* (*CFAR*) [4]. This rule is effective, since the false alarm costs a large penalty in the acquisition time, and the detection threshold for a low CFAR leads to the optimal acquisition performance (i.e., minimum MAT μ_T or MAC μ_C) for GNSS signals with moderate and high SNR. Note that the MAT μ_T and MAC μ_C are functions of γ, P_d, P_m, P_f, penalty time, N_{Hc}, N_{Hf}, N_i, and T_{co}, and that the minimum $\mu_{T,\min}$ and the minimum $\mu_{C,\min}$ can be found by letting the derivative of μ_T and μ_C with respect to γ be equal to zero, respectively. However, in [16], it is found that the algebraically determined optimal detection threshold γ achieves smaller MAT μ_T and MAC μ_C than the CFAR-based detection threshold for weak GNSS signals. Note that, to determine γ for all of the detection variables except MTSMR, knowledge of the average integration function output at incorrect hypotheses $E[Z \mid H_0]$ (in other words, noise power in the integration output) is required.

Other factors affecting the GNSS acquisition performance

In addition to the detection variable, search strategy, and detection scheme, the acquisition performance depends on a number of other factors. There are receiver-dependent factors, such as front-end filtering, sampling rate f_s, oscillator stability, and quantization levels, and there are receiver-independent factors such as multipath and NLOS, interference signals, user dynamics,

code Doppler, ionospheric and tropospheric delays, and the C/N_0 of the incoming signal [2]–[4]. Among the receiver-dependent factors, the sampling rate and oscillator stability are the critical design factors in the achievement of low computational cost and fast GNSS signal acquisition. Since $N_{co} = f_s T_{co}$, a higher sampling rate increases N_{co}, which increases the SNR (i.e., the postcorrelation SNR) at the integration function output, but the MAC μ_C increases at the same time. On the other hand, when T_{co} becomes too long for the low-cost quartz crystal oscillator used in many GNSS receivers [18], the frequency drift during T_{co} degrades the postcorrelation output (i.e., at the integration function output) SNR. In addition to the aforementioned factors, the parameters of the signal structure, such as data-bit width, modulation scheme, secondary code, and relative power allocation between the pilot and data channels, have a strong influence on the acquisition complexity.

Challenges for weak GNSS signal acquisition

Figure 4 shows a normalized complete search result made by the conventional GPS L1 C/A search technique for $T_{co} = 1$ ms and $N_i = 1$, where the true hypothesis H_1 is at $\kappa = 1,226$ and $\lambda = 11$. As shown, there are some noticeable false peaks in the search result (i.e., relatively large $Z \mid H_0$'s), which may cause false alarms when the signal peak (i.e., the integration output at the correct hypothesis $Z \mid H_1$) is relatively small compared to the noise peaks. In fact, the false peaks are from the nonzero output of the autocorrelation at nonzero delays and from the noise in the received signal. In practice, the size of the false peaks can be suppressed by using larger N_{co} and N_i. However, increasing N_{co} is restricted by the data-bit transition, and increasing N_i is less effective and costs much larger MAT than increasing N_{co}. As an example, when $N_t = N_i N_{co}$ signal samples are used, a coherent integration technique produces a signal peak power proportional to N_t^2, while a noncoherent integration technique results in signal peak power proportional to $N_i N_{co}^2$. Therefore, the coherent integration technique produces N_i times higher signal peak power than the noncoherent technique. However, the coherent integration technique requires a longer acquisition time and higher computational complexity than the noncoherent technique due to the increased number of Doppler-frequency hypotheses by N_i times. For the FFT-based technique in Figure 3, the total numbers of complex multiplications for the coherent and noncoherent integration techniques are $N_t(4\log_2 N_t + 7)$ and $N_t(4\log_2 N_{co} + 7)$, respectively, for each Doppler-frequency hypothesis, and the coherent integration technique has N_i times more Doppler-frequency hypotheses to test. Consequently, improving the GNSS acquisition sensitivity for weak signals conflicts with another primary goal of GNSS receivers—low acquisition complexity. Therefore, a tradeoff between the sensitivity and acquisition complexity should be necessary for mass-market GNSS receivers; however, achieving the two goals at the same time is still a challenge in the development of high sensitivity GNSS receivers.

Channel combining techniques for new GNSS signals

This section introduces channel-combining (in other words, joint channel acquisition) techniques for new GNSS signals. The channel-combining techniques are employed by the integration function $G(\cdot)$ in Figure 1, which combines the signal power carried in the pilot and data channels or the power of GNSS signals at different frequencies to improve the acquisition sensitivity.

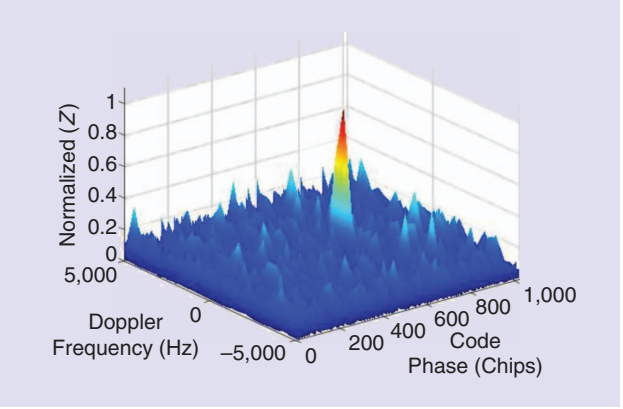

FIGURE 4. A complete search result over the 2-D plane.

Channel structure of new GNSS signals

Many of the new GNSS signals have composite channel structure to accommodate the data-free (i.e., pilot) and data channels, which are separated by 90° phase shift (1b), orthogonal codes (1c), and time-division multiplexing (TDM) (1c). For example, GPS L5 uses QPSK modulation and both Galileo E5a and E5b can be represented by QPSK-modulated signals; GPS L1C, Galileo E1 OS, and (candidate) BeiDou B1 utilize orthogonal codes; and GPS L2C has the TDM scheme, to transmit the two channels separately.

When an incoming GNSS signal has a composite channel structure, the acquisition function may utilize the integration function $G(\cdot)$ to combine the signal power in the pilot and data channels to increase the acquisition sensitivity. (Note that $G(\cdot)$ may be only used for the pilot channel depending on the target acquisition sensitivity.) However, the usage of channel combining increases the acquisition complexity and the benefit may be small when most of the signal power is in the pilot channel. In addition, when most of the signal power is in the low frequency component (relative to the center frequency), e.g., sinBOC(1,1), and the rest is in the high frequency component, e.g., sinBOC(6,1), combining the two frequency components may improve the acquisition sensitivity slightly, while the acquisition complexity may be increased significantly, where sinBOC(m,1) represents $\text{sign}[\sin(2\pi m R_c t)]$. In the following, we introduce the channel-combining techniques for new GNSS signals in (1b) and (1c).

Channel-combining techniques for QPSK-modulated GNSS signals

Some of the new GNSS signals, such as GPS L5 and Galileo E5a and E5b, have the QPSK modulation for pilot and data channels with equal power. Therefore, it can be useful to combine the signal powers in the two channels using the integration function $G(\cdot)$. There are a few channel-combining techniques for pilot and

data channels in QPSK modulation, such as noncoherent, semicoherent, and differentially coherent combining techniques [19].

Noncoherent channel combining

Noncoherent channel combining simply adds the magnitudes (or magnitudes squared) of the correlation outputs of the pilot and data channels [20]. Similar to the noncoherent integration technique, noncoherent channel-combining technique provides a relatively small SNR increase comparing to the coherent combining technique and may suffer from the squaring loss [3].

Semicoherent channel combining

Since the relative phase between the data channel and the pilot channel is either $+90^\circ$ or -90° due to the unknown data and the secondary codes modulating the channels, the integration function output in a complex form can be expressed with one of the two combinations: $R_D + jR_P$ and $R_D - jR_P$, where $R_D (= R_D^I + jR_D^Q)$ and $R_P (= R_P^I + jR_P^Q)$ are the correlation outputs of data and pilot channels, respectively, and the superscripts I and Q represent the in-phase and quadrature-phase components, respectively (see Figure 1). Therefore, in the semicoherent combining, the integration function $G(\cdot)$ returns the combination result of larger magnitude (or magnitude squared) between the two. In practice, the semicoherently combined output can be noncoherently integrated to produce the detection variable [19].

Differentially coherent channel combining

Denoting the unknown phase of the data and pilot channels as φ and $\varphi \pm 90^\circ$, respectively, multiplying the data channel correlation output, R_D, with the complex conjugate of the pilot channel correlation output, R_P^*, results in an imaginary component (i.e., the resulting phase becomes $\mp 90^\circ$). Therefore, in [19], the detection variable with differentially coherent combining is obtained from the magnitude of the imaginary component of the result, i.e., $|Im\{R_D R_P^*\}|$, where $Im\{\cdot\}$ is a function returning the imaginary part.

Coherent channel combining and integration for optimal detection

In fact, the semicoherent combining technique and the differentially coherent combining technique are only suboptimal detection techniques, since they estimate the relative signs between the data and pilot channels and between two consecutive correlation outputs. In the study of the optimal detection technique for GPS L5 signal [21], it is indicated that the optimal detection technique should utilize all of the constraints given by the data bit and secondary codes for the coherent channel combining and the coherent integration of correlation outputs. Therefore, the optimal detection technique for weak GNSS signals requires an additional search for the secondary code and data bits along the third dimension indexed with η in (3). This may be an exhaustive search, since the number of possible data bits and code-chip combinations grows exponentially with $N_t (= N_i T_{co})$. When the consecutive correlation outputs are obtained within the same data bit, the optimal search technique for GPS L5 signals may only need to perform an additional search for the secondary code, the Neuman–Hoffman (NH) code. To reduce the additional search complexity for the secondary code, a tree structure of the NH code may be utilized [22], and the characteristic code of the NH code that has all of the possible code-chip transition patterns can be used [23]. Table 3 summarizes the detection variables of the channel-combining techniques.

Channel combining technique for in-phase GNSS signals

GPS L1C, Galileo E1 OS, and (candidate) BeiDou B1 signals have the pilot and data channels that are separated by the spreading codes and transmitted (mostly) in the same phase (i.e., in-phase) channel. Note that the candidate BeiDou B1 pilot channel has a QMBOC modulation, in which a small portion (about 12%) of its power is allocated to the sinBOC(6,1)-modulated high-frequency component in the quadrature phase. However, the advantage of combining the two channels to improve the acquisition sensitivity possibly can be small when the signal power is not evenly distributed between the two channels [23]. In addition, combining the two channels increases the receiver complexity considerably. For example, the GPS L1C and (the candidate) BeiDou B1 have 75% of their signal power in the pilot channel, and the remaining 25% is in the data channel. The acquisition performance, in terms of the detection probability in the individual hypothesis test, P_d, when the only pilot channel is used is slightly lower than that when the both channels are used. In addition, since the pilot channels of GPS L1C and (the candidate) BeiDou B1 have about 88% of the total signal power in the sinBOC(1,1) and the remaining 12% in sinBOC(6,1), a receiver may neglect the sinBOC(6,1) component and processes only the signal component in sinBOC(1,1) at the cost of small sensitivity loss; 1.1 dB for GPS L1C and 0.56 dB for (the candidate) BeiDou B1 signals.

GPS L2C signal has a TDM of data-modulated civil moderate (CM) code and data-free civil long (CL) code of $T_p = 20$ ms and $T_p = 1.5$ s, respectively. Since the two channels are separated in time and the CL

Table 3. Detection variables of various channel-combining techniques.

Channel Combining	Detection variable for the κth code phase and λth Doppler-frequency hypothesis
Noncoherent	$Z_{\text{ncc}}[\kappa,\lambda] = \sum_{\eta=0}^{N_i-1} \{\lvert R_D[\eta,\kappa,\lambda]\rvert^2 + \lvert R_P[\eta,\kappa,\lambda]\rvert^2\}$
Semicoherent	$Z_{\text{scc}}[\kappa,\lambda] = \sum_{\eta=0}^{N_i-1} \max\{\lvert R_+[\eta,\kappa,\lambda]\rvert^2,\ \lvert R_-[\eta,\kappa,\lambda]\rvert^2\}$, where $R_\pm[\eta,\kappa,\lambda] = R_D[\eta,\kappa,\lambda] \pm jR_P[\eta,\kappa,\lambda]$
Differentially coherent	$Z_{\text{dcc}}[\kappa,\lambda] = \sum_{\eta=1}^{N_i-1} \lvert \text{Im}\{R_D[\eta,\kappa,\lambda] R_P^*[\eta,\kappa,\lambda]\}\rvert$
Coherent	$Z_{\text{cc}}[\kappa,\lambda] = \max_{I} \left\lvert \sum_{\eta=0}^{N_i-1} D[\eta] S_D[\eta] R_D[\eta,\kappa,\lambda] + jS_P[\eta]\, R_P[\eta,\kappa,\lambda] \right\rvert^2$, where $I = \{\{D[\eta]S_D[\eta], S_P[\eta]\} \lvert \eta = 0,1,2,\ldots,N_i-1\}$

code acquisition requires a high acquisition complexity due to the long code length, some GPS L2C acquisition techniques leverage CM code acquisition to acquire the CL code [24]; once the CM code is acquired, there are only 75 CL code-phase hypotheses left. In some studies [25], [26], partial correlation algorithms are utilized to reduce the computational cost in the FFT-based technique for L2C signals (introduced in the section "Low Computational Techniques Achieving Fast Acquisition and High Sensitivity"), and, in [6], MGDC is used for a partial acquisition of L2C signals.

In the case of the Galileo E1 OS, E5a, and E5b and GPS L5 signals, the pilot and data channels have an equal signal power, which makes it effective to combine both channels for higher acquisition sensitivity [20], [27], [28]. For Galileo E1 OS signals, however, both channels have sinBOC(1,1) and sinBOC(6,1) components carrying about 91% and 9% of the total signal power, respectively. Therefore, it may be useful and efficient for a receiver acquiring Galileo E1 OS signals to utilize both channels with the sinBOC(6,1) component neglected to reduce the acquisition complexity.

Channel-combining technique for GNSS signals at different frequencies

Since there are GNSS satellites synchronously transmitting ranging signals at different frequencies, a receiver can make use of all available signals from the same satellite for increased sensitivity and higher positioning accuracy. In [29], a Galileo receiver is developed to acquire both Galileo E5a and E5b signals coherently, for which it is exploited that the data-bit and code-chip boundaries are synchronized between the two signals, the code delays of the two signals are the same, and the Doppler-frequency ratio between E5a and E5b signals is the same to the carrier frequency ratio between E5a and E5b. Exploiting the same assumption, a dual frequency receiver for coherent acquisition of GPS L1 C/A and GPS L2C signals is developed and demonstrated successfully [30].

Low computational techniques achieving fast acquisition and high sensitivity

While higher acquisition sensitivity can be achieved by increasing N_i and N_{co} and by channel combining in $G(\cdot)$, low computational fast acquisition techniques are of great interest when $N_t (= N_i N_{\text{co}} = f_s T_t)$ should be too large and very long coherent integration is inevitable. There have been a number of techniques introduced in the literature to reduce the huge computational cost and the large MAT required by the conventional time-domain and frequency-domain (i.e., FFT-based) correlation techniques for increased sensitivity. This section focuses on some of the recent signal processing techniques for high sensitivity and fast acquisition.

Among a large number of various low computational, high sensitivity, and fast acquisition techniques, we investigate techniques in three categories: sample-domain techniques, frequency-domain techniques, and assisted acquisition techniques. Averaging techniques are introduced as well-known sample-domain techniques, where a receiver reduces the size of the signal samples and employs specialized search strategies to cope with the timing and frequency uncertainties caused by the sample reduction. For frequency-domain techniques, recent fast computation algorithms enabling huge computational cost reduction are introduced. All of the frequency-domain techniques utilize data-segmentation schemes, specialized signal processing, and specialized search strategies. Note that the signal processing techniques and search strategies used in both the sample- and frequency-domain techniques are different from those in the conventional techniques discussed in the sections "Fundamentals of GNSS Signal Acquisition" and "Channel Combining Techniques for New GNSS Signals." The assisted acquisition techniques represented by the assisted-GNSS (A-GNSS) are introduced as one of the most widely used recent techniques in comparison to both the sample- and frequency-domain techniques that are for standalone GNSS receivers.

Also note that there are different kinds of low computational, fast acquisition techniques not introduced in this article. For example, hypothesis compression techniques compress the 2-D hypothesis plane into a much smaller compressed hypothesis plane and perform a quicker search over the compressed hypothesis plane [11]. There are multisatellite maximum likelihood (MS-ML) acquisition techniques [31] that can acquire multiple satellite signals simultaneously. In practice, the hypothesis compression techniques suffer from SNR degradation with respect to the compression rate, and the recent MS-ML techniques require a fine time and frequency assistance or may require a huge computational cost.

Sample-domain techniques: Averaging techniques

Averaging techniques are used to reduce the number of signal samples to process in the GNSS signal acquisition. The averaging process can be performed over neighboring (consecutive) signal samples or over the blocks of signal samples, which results in a larger ambiguity of timing than processing the original samples or results in a loss of signal energy when the averaged signal samples from different blocks have different phases, respectively. To mitigate these side effects, the averaging techniques have to employ additional signal processing techniques with search strategies different from the conventional techniques.

Averaging correlation technique

When the sampling rate is very high (i.e., $f_s \gg 2R_c$) and there are too many signal samples to be processed with the time-domain correlation or the FFT-based techniques, the averaging correlation (AC) technique [32] can be useful to reduce the number of signal samples by taking the average of every $N_{\text{sc}} (\le f_s T_c)$ consecutive samples of $y_B[n]$, where $y_B[n]$ is the Doppler-frequency compensated samples in Figure 1. The receiver replica $x[n]$ is generated at a reduced rate f_s/N_{sc} accordingly, so that the correlation length and the size of the FFT and IFFT become N_{sc} times smaller. However, when the averaged sample is constructed of signal samples across a chip boundary, signal samples belonging to the neighboring chips may cancel each other and cause an SNR loss in the correlation output. Therefore, only the signal samples within the same code chip should be averaged to maximize the SNR. In this technique, N_{sc} sets of averaged sample sequences with different sample offsets are generated first, and each set is

used in the search of incoming signals independently. As a result, there are N_{sc} maximum integration outputs for N_{sc} sets, and the largest one is used as the detection variable. In FFT-based techniques, the AC technique performs (N_t/N_{sc})-point FFTs and IFFTs by N_{sc} times for each Doppler-frequency hypothesis, and there are $N_t[4\log_2(N_t/N_{sc})+7]$ complex multiplications for each of $2\lceil 2f^D_{\max}T_t\rceil+1$ Doppler-frequency hypotheses, resulting in a total complexity of $O(N_i^2 N_{Hf_1} N_{co}\log_2(N_t/N_{sc}))$, where $N_{Hf_1}=2\lceil 2f^D_{\max}T_1\rceil+1$.

Block averaging preprocessing technique

The block averaging preprocessing (BAP) technique [33] takes the average of the Doppler-frequency compensated signal samples $y_B[n]$ separated by T_p (i.e., one period). For an example of GPS L1 C/A signals, $T_p=T_1$ (= 1 ms), and the incoming signal samples are recorded row-by-row in a data matrix Q of size $[N_i^1\times N_1]$, where $N_i^1=N_t/N_1$ and $N_1=f_sT_1$, and then columns of Q are averaged to build an averaged data block of size $[1\times N_1]$. It is assumed that the data bit in the incoming signal is already wiped off and that when the remaining Doppler frequency in $y_B[n]$ is an integer multiple of $1/T_1(=1$ kHz), samples of the same column have the same phase so that they can be coherently accumulated. Consequently, the technique has two steps of Doppler-frequency search:

- step 1: a fine search over [0, 1] kHz with a search step size $\delta f=1/(2N_iT_1)$
- step 2: a coarse search over $[-f^D_{\max}, f^D_{\max}]$ with a larger search step size $\Delta f=1/T_1$.

Therefore, there are N_i-fine frequency hypotheses in step 1, and when a signal peak is found at, e.g., $\lambda_1\delta f$, step 2 performs a coarse Doppler-frequency search for N_{Hf_1} Doppler-frequency hypotheses at $\lambda_1\delta f+[-f^D_{\max}+\Delta f,\ -f^D_{\max}+2\Delta f,\ldots,f^D_{\max}]$. As a result, there are $N_t(N_i+N_{Hf_1})$ complex multiplications for preprocessing and N_i and N_{Hf_1} times N_1-point FFT-based correlations for the first and second steps, respectively, which results in an overall complexity of $O(N_tN_i+(N_i+N_{Hf_1})N_1\log_2N_1)$.

Frequency-domain techniques: Fast computation algorithms

Recent fast computation algorithms are mostly for the FFT-based technique when the coherent integration interval $T_{co}(\gg T_1)$ is too long and N_{co} becomes huge. Therefore, the problem is not just in the huge size of FFT operations, but also in the huge number of Doppler-frequency hypotheses to test. In general, the algorithms make use of the repetition of the GNSS spreading codes in the received signal samples to reduce the size of the FFT operations by forming a matrix with the signal samples and applying row-wise and column-wise FFT/IFFT operations. Similar to the BAP technique, processing GNSS signal samples in a matrix form requires a specialized Doppler-frequency search strategy different from the conventional search strategies. This section introduces these algorithms in detail to show the signal processing and specialized search strategies required for each.

Two-dimensional FFT-based technique

The 2-D FFT-based technique (2-D-FFT technique, for short) [12] is based on the similar idea used in the BAP technique in Figure 3. Similar to the Q matrix in the BAP technique, the 2-D-FFT technique uses $R(=Q^T$, i.e., a signal matrix recorded column-by-column) to perform a fine Doppler-frequency search over [0, 1] kHz with a search step δf and then a coarse Doppler-frequency search with $\Delta f=1$ kHz search step size over $[-f^D_{\max}, f^D_{\max}]$. The 2-D-FFT technique applies row-wise and column-wise FFT's to the data matrix R to perform the fine and coarse searches, however, each search process requires additional phase compensations to the resulting matrix after the FFT operations.

Figure 5 shows the 2-D-FFT technique, and the data matrix R of size $[N_1\times N_i^1]$ is built by filling R with $y[n]$ column-by-column. For the fine search, N_i^1-point FFT is applied to each row of R to yield R_1 (see Figure 5), because each row of R has signal samples collected at every T_1 seconds over the total T_t seconds. In fact, the actual correlation should be the multiplications between the columns of R_1 and X (i.e., the FFT of the spreading code); however, the columns of R_1 are different from the FFT columns of R. This difference can be compensated for by an element-by-element multiplication with the matrix C and the diagonal matrix M^* in the second and the sixth steps, respectively. The third and the fourth steps are for the multiplication of the fine-Doppler-frequency compensated signal $y[n]$ with the coarse-Doppler-frequency compensated signal $x[n]$ in the frequency domain. Denoting R_2, R_3, and X as the result of the second step, the column-wise FFT of R_2 and the N_1-point FFT output of $x[n]$, respectively, multiplication of the complex conjugate of the circular shifted

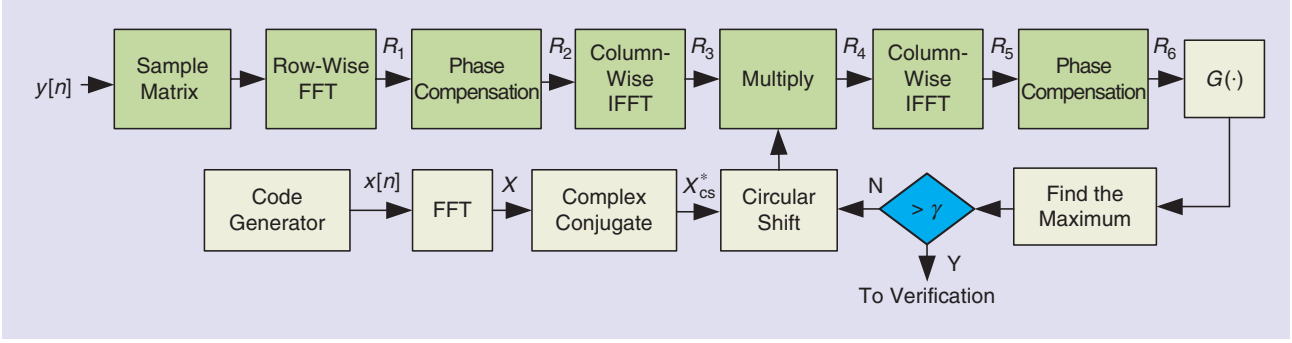

FIGURE 5. Fast FFT-based technique for data in a matrix form.

X, X^*_{cs}, to each column of R_3 results in R_4. The fifth step applies column-wise IFFT to each column of R_4 to yield R_5, and, in the sixth step, R_5 is multiplied with a diagonal phase-compensation matrix M^* to complete the frequency shift in unit of 1 kHz. As a result, the overall complexity in the number of complex multiplications is about $O(N_{\text{Hf}} N_t \log_2 N_1)$. Note that the green blocks in Figure 5 are required for the new signal processing algorithm of the 2-D-FFT technique and, also, that the technique assumes that $y[n]$ is data free (i.e., wiped off). This is the same assumption used for the BAP technique, which limits the application of the technique in practice. However, the 2-D-FFT technique requires much lower computational cost than the BAP technique.

FFT-based partial correlation technique

When the spreading code period is too long and computationally expensive to use the FFT-based technique, the FFT-based partial correlation that obtains partial correlation outputs utilizing signal segments can be effective. In [25] and [26], the segmented FFT computation algorithm is devised for the FFT-based long coherent correlation of the GPS L2-CL signals in four steps. In the following, it is assumed that the incoming signal $y(t)$ and receiver replica $x(t)$ are sampled and collected over a long code period $T_P (= T_t)$ and then divided into N_i segments, and that each segment $(k = 1, 2, \ldots, N_i)$ has N_{co} samples over T_{co}, i.e., $T_t = N_i T_{\text{co}}$.

The first two steps are for FFT-based correlation between $y[n]$ and $x[n]$ with zero-padding. Let y_k and x_k be the kth segment of incoming signal samples and that of spreading code samples, respectively. In the first step, y_k is zero-padded and fast Fourier transformed to obtain Y_k for all k, and, in the second step, pairs of consecutive x_k (i.e., $[x_1, x_2]$, $[x_2, x_3]$, …, $[x_{N_i-1}, x_{N_i}]$, $[x_{N_i}, x_1]$) are fast Fourier transformed to obtain X_{rl} for $r, l \in \{1, 2, \ldots, N_i\}$. The third step performs the IFFT of $Y_k (X_{\text{rl}})^*$ for all $r, l \in \{1, 2, \ldots, N_i\}$ and $k \in \{1, 2, \ldots, 2N_i\}$, and takes the first N_{co} elements of each IFFT output to obtain the partial correlation output $R_{k,r} = y_k \circledast x_r$. Since the lth partial segment of the complete coherent circular correlation output (between the $N_i N_{\text{co}}$ signal samples y and $N_i N_{\text{co}}$ spreading code samples x) can be obtained from the point-by-point summation of N_i IFFT outputs, i.e., $\Sigma_{k=1}^{N_i} R_{l+k-1,k}$, the complete coherent integration result is found by concatenating the partial segments for all $l = 1, 2, \ldots, N_i$ in the fourth step. Also, note that the third and fourth steps can be repeated for circular shifted Y_k, since the circular shift of Y_k by one sample is a Doppler-frequency shift by $\Delta_f = 1/(2T_{\text{co}})$ of the incoming signal. However, the circular shift in the unit of Δ_f is only a coarse search. To perform the fine search, a carrier signal of frequency δf is multiplied to the incoming signal for frequency compensation and then performs the aforementioned four-step algorithm with the frequency compensated signal. In [26], multiple δf values are selected uniformly in $[-1/(4T_{\text{co}}), 1/(4T_{\text{co}})]$ for every coarse search step. In practice, there can be N_i fine-search hypotheses and $2\lceil 2 f^D_{\max} T_{co} \rceil (\cong 400$ for GPS L2-CL) coarse search hypotheses. As a result, the overall computational complexity has an order of $O(\lceil f^D_{\max} T_{co} \rceil N_i N_t \log_2 N_{\text{co}})$.

SDHT-based fast acquisition technique

The synthesized Doppler-frequency hypothesis testing (SDHT) technique [34] in Figure 6 exploits the idea that a long coherent integration (over multiple code periods) output for a Doppler-frequency hypothesis at $(\lambda + (1/2))\Delta f$ can be estimated exploiting consecutive short (i.e., one period) coherent integration outputs at a neighboring Doppler-frequency hypothesis at $\lambda \Delta f$ or at $(\lambda + 1)\Delta f$, where the estimation requires a phase-compensation process and does not require actual correlations. Note that the alternative estimation scheme exploiting both of the neighboring Doppler-frequency hypotheses can lower the computational cost slightly more [34] but may increase ambiguity due to the inverse cosine function. The SDHT technique can be useful, when a receiver tries to double the coherent integration length (i.e., $N_i = 2$) for higher sensitivity. Using GPS L1 C/A as an example, when a receiver obtained N_1 signal samples over $T_1 (= T_p = 1$ ms) and has performed coherent correlations with $T_{\text{co}} = T_1$ for every Doppler-frequency hypothesis at every 500 Hz within [–5, 5] kHz (for example, –5,000 Hz, –4,500 Hz, –4,000 Hz, … 5,000 Hz) but no signal peak is found, the receiver may need to double the coherent

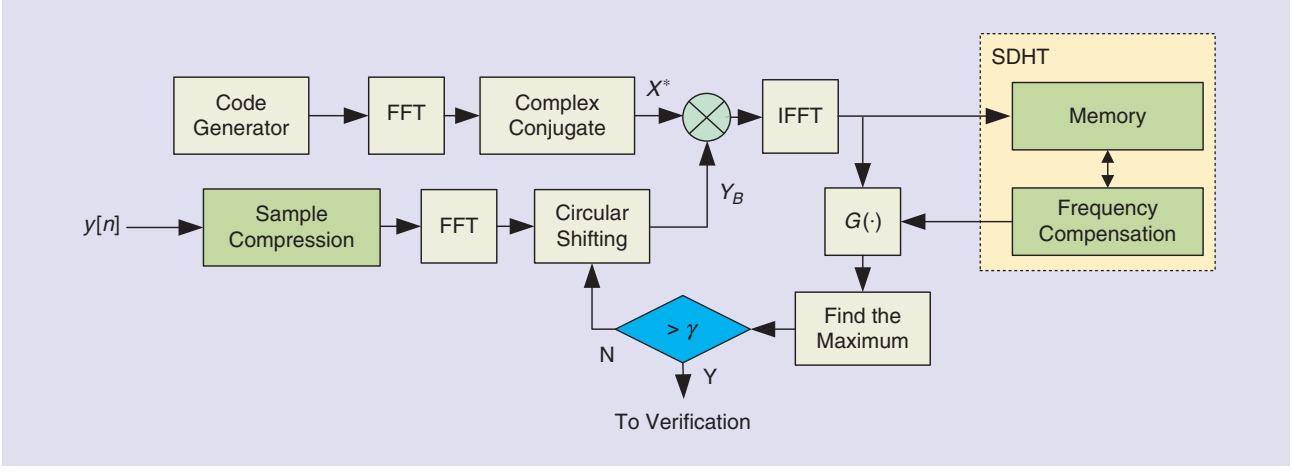

FIGURE 6. The SDHT-based fast acquisition technique. The green blocks are required algorithms to the FFT-based technique in Figure 3.

integration length to $2T_1$. In such a case, a receiver employing the SDHT technique utilizes the next N_1 signal samples to perform an additional coherent search with $T_{co} = T_1$ for the same tested Doppler frequencies and coherently adds the results to the previous correlation results to obtain the coherent correlation output for $N_i = 2$ at the same tested Doppler-frequency hypotheses. When no signal is found yet, the receiver can find coherent correlation output for Doppler frequencies in between the above-tested Doppler frequencies (i.e., –4,750 Hz, –4,250 Hz,…, 4,750 Hz). As a result, the receiver obtains coherent correlation output for $T_{co} = 2T_1$ at all Doppler-frequency hypotheses at every 250 Hz within [–5, 5] kHz. This process can be repeated for $N_i = 4, 8,\ldots$, until the receiver detects the signal. In [34], a sample averaging technique is also utilized in the SDHT technique and achieves a lower computational cost than the 2-D-FFT technique. It should be noted that since the SDHT technique does not assume data-free (wiped-off) signal samples and finds consecutive correlation outputs $R[\eta,:,:]$ for $\eta = 1, 2, \ldots$, it is possible to apply the data bit search process to the result of the SDHT technique.

Assisted acquisition technique

To enhance the acquisition sensitivity and to reduce the time-to-first-fix (time to make a first position fix in a cold start) of GNSS receivers connected to the cellular networks through mobile phones, the GNSS receivers can make use of GNSS signal observations made by the network. This is possible in the A-GNSS technique that is a high sensitivity and fast acquisition technique different from those techniques for standalone GNSS receivers introduced in the sections "Sample-Domain Techniques: Averaging Techniques" and "Frequency-Domain Techniques: Fast Computation Algorithms." There is various assistance in the A-GNSS technique, including acquisition assistance to help the mobile GNSS receiver (i.e., A-GNSS receiver) narrow down the search area much smaller than the whole 2-D hypothesis plane, and the conventional correlation techniques and search strategies in the sections "Fundamentals of GNSS Signal Acquisition" and "Channel Combining Techniques for New GNSS Signals" can be applied. This section introduces the assisted acquisition in the A-GNSS technique and some technical issues with the recent cellular networks such as long-term evolution (LTE).

In the A-GNSS technique [35], the assistance generated by the assistance server equipped with a reference GNSS station is to help the A-GNSS receivers for acquisition and positioning. The acquisition assistance sent to the A-GNSS receiver includes the satellite ID, expected Doppler frequency and Doppler rate, Doppler uncertainty, code phase, integer code phase (the number of code periods from the last bit boundary), code-phase search window, GPS bit number, azimuth, and elevation [36]. These are the essential information elements (IEs) needed to indicate (with uncertainties) the prompt Doppler frequency and the prompt code phase of the GNSS signal being observed at the remote A-GNSS receiver. These IEs make it possible for the acquisition function in the A-GNSS receiver to narrow the search space down to a small, local search space composed of a small number of hypotheses. As a result, the technique improves the acquisition performance significantly in terms of speed and complexity. Other assistance for positioning includes the reference time, reference location (usually, the base station location), differential corrections, navigation model (i.e., satellite ephemeris and clock corrections), ionospheric model, coordinated universal time model, and real-time integrity [36].

In practice, there are two operational modes of the A-GNSS technique: the mobile station (MS) assisted and the MS based. In the MS-assisted mode, an A-GNSS receiver acquires and measures the incoming GNSS signals and the measurements are sent to the network for position calculations, whereas in the MS-based mode, an A-GNSS receiver not only acquires and measures the incoming GNSS signals, but also calculates its own position [37]. However, the acquisition assistance is only delivered in the MS-assisted mode. In the MS-based mode, a mobile phone can download the other assistance data from the assistance server in advance, so that the A-GNSS receiver can exploit the data to narrow down the search space [3].

While the principle of A-GNSS technique has been standardized accordingly through the generations of cellular networks, it should be noted that the performance benefit from the acquisition assistance strongly relies on the clock and frequency accuracies of the downlink pilot signal. In the cellular networks synchronized to GPS, such as second-generation code-division multiple access (2G CDMA) and LTE in time-division duplexing mode, the (downlink) pilot channel and the cell-specific reference signal can be used as a fine frequency reference to stabilize the mobile phone oscillator and to narrow down the Doppler-frequency search range. The pilot channel and cell-specific reference are also used as an accurate time reference to narrow the code-phase search range. In this case, an A-GNSS receiver, determining a smaller search space using the assistance, may only need to consider the Doppler-frequency uncertainties due to the user motion. Note that the code-phase uncertainty due to the downlink propagation is included in the assistance information. On the other hand, in the asynchronous cellular networks (to GNSS) such as wideband-CDMA and LTE in the frequency-division duplexing mode [38]–[40], the Doppler-frequency uncertainty to define the search space needs to be large enough, and the prompt code phase information in the acquisition assistance may be not accurate.

Conclusions and future directions

To meet the growing demands for GNSS positioning in GNSS-challenged environments, high sensitivity and fast acquisition have become the two most desired features for GNSS receivers. First introduced were the fundamentals of the GNSS acquisition function and some of the new acquisition techniques for new GNSS signals composed of pilot and data channels in QPSK or in the same phase. In the second part, we have investigated fast GNSS acquisition techniques, which achieve both low computational cost and high sensitivity, for standalone GNSS and A-GNSS receivers. It has been found that the fast GNSS acquisition techniques use specialized search strategies according to their

signal processing algorithms. As discussed in relation to the state-of-the-art acquisition techniques in this article, signal processing techniques for higher sensitivity and faster acquisition are still under development with the goal of delivering reliable positioning performance in the GNSS-challenged environments. However, GNSS acquisition technologies are also evolving rapidly, and new GNSS signals will become available in the near future. Accordingly, GNSS positioning in GNSS-challenged environments is expected to become more reliable and accurate, making GNSS more useful for indoor LBSs.

Acknowledgment

This research was supported by the Basic Science Research Program through the National Research Foundation of South Korea funded by the Ministry of Science, ICT, and Future Planning (2017R1A2B2010635).

Author

Seung-Hyun Kong (skong@kaist.ac.kr) received his B.S. degree in electronics engineering from Sogang University, South Korea, in 1992, his M.S. degree in electrical engineering from Polytechnic University, New York, in 1994, and his Ph.D. degree in aeronautics and astronautics from Stanford University, California, in 2006. He has been with the Korea Advanced Institute of Science and Technology, Daejeon, South Korea, since 2010, where he is currently an associate professor at the CCS Graduate School of Green Transportation. He is an editor of *IET Radar, Sonar & Navigation* and an associate editor of *IEEE Transactions on Intelligent Transportation Systems* and *IEEE Access*. His research interests include signal processing for global navigation satellite systems, neutral networks for sensing, and vehicular communication systems. He is a Senior Member of the IEEE.

References

[1] D. N. Hatfield, "A report on technical and operational issues impacting the provision of wireless enhanced 911 services," Tech. Rep., Federal Communications Commission, 2002.

[2] E. D. Kaplan and C. J. Hegarty, *Understanding GPS: Principles and Applications*, 2nd ed. Norwood, MA: Artech House, 2005.

[3] F. Van Diggelen, *A-GPS: Assisted GPS, GNSS, and SBAS*. Norwood, MA: Artech House, 2009.

[4] B. W. Parkinson and J. J. Spilker, Jr., *Global Positioning System: Theory and Applications, Volume I and II*. Plymouth, MA: AIAA, 1996.

[5] M. Foucras, U. Ngayap, F. Bacard, and B. Ekambi, "Acquisition performance comparison of new generation of GNSS BOC-modulated signals," in *Proc.* 29th *Int. Tech. Meeting, ION GNSS+ 2016*, Portland, OR, Sept. 2016, pp. 107–119.

[6] J. A. Ávila Rodriguez, T. Pany, and B. Eissfeller, "A theoretical analysis of acquisition algorithms for indoor positioning," in *Proc. 2nd ESA Workshop on Satellite Navigation User Equipment Technologies NAVITEC*, Noordwijk, The Netherlands, Dec. 2004.

[7] T. H. Ta, S. U. Qaisar, A. G. Dempster, and F. Dovis, "Partial differential postcorrelation processing for GPS L2C signal acquisition," *IEEE Trans. Aerosp. Electron. Syst.*, vol. 48, no. 2, pp. 1287–1305, Apr. 2012.

[8] G. E. Corazza and R. Pedone, "Generalized and average likelihood ratio testing for post detection integration," *IEEE Trans. Commun.*, vol. 55, no. 11, pp. 2159–2171, Nov. 2007.

[9] F. Dovis and T. H. Ta, "High sensitivity techniques for GNSS signal acquisition," in *Global Navigation Satellite Systems: Signal, Theory and Applications*, J. Shuanggen, Ed. InTech, 2012.

[10] A. J. Viterbi, *CDMA: Principles of Spread Spectrum Communication*. Reading, MA: Addison-Wesley, 1995.

[11] B. Kim and S.-H. Kong, "Design of FFT-based TDCC for GNSS acquisition," *IEEE Trans. Wireless Commun.*, vol. 13, no. 5, pp. 2798–2808, 2014.

[12] D. Alkopian, "Fast FFT based GPS satellite acquisition methods," *IEE Proc. Radar Sonar Navigat.*, vol. 152, no. 4, pp. 277–286, Aug. 2005.

[13] D. Borio, "Impact of GPS acquisition strategy on decision probabilities," *IEEE Trans. Aerosp. Electron. Syst.*, vol. 44, no. 3, pp. 996–1011, July 2008.

[14] G. E. Corazza, "On the MAX/TC criterion for code acquisition and its application to DS-SSMA systems," *IEEE Trans. Commun.*, vol. 44, no. 9, pp. 1173–1182, Sept. 1996.

[15] B. Geiger, C. Vogel, and M. Soudan, "Comparison between ratio detection and threshold comparison for GNSS acquisition," *IEEE Trans. Aerosp. Electron. Syst.*, vol. 48, no. 2, pp. 1772–1779, Apr. 2012.

[16] B. Kim and S.-H. Kong, "Determination of detection parameters on TDCC performance," *IEEE Trans. Wireless Commun.*, vol. 13, no. 5, pp. 2422–2431, May 2014.

[17] S. F. Rounds and C. Norman, "Combined parallel and sequential detection for improved GPS acquisition," in *Proc. ION/IAIN World Congr. Assoc.*, June 2000, San Diego, CA, pp. 368–372.

[18] P. W. Ward, "GPS receiver search techniques," in *Proc. IEEE Position Location Navigation Symp.*, Atlanta, GA, Apr. 1996, pp. 604–611.

[19] D. Borio, C. O'Driscoll, and G. Lachapelle, "Composite GNSS signal acquisition over multiple code periods," *IEEE Trans. Aerosp. Electron. Syst.*, vol. 46, no. 1, pp. 193–206, Jan. 2010.

[20] F. Bastide, O. Julien, C. Macabiau, and B. Roturier, "Analysis of L5/E5 acquisition, tracking and data demodulation thresholds," in *Proc. 15th Int. ION Global Positioning Syst. Tech. Meeting 2002*, Portland, OR, Sept. 2002, pp. 2196–2207.

[21] C. J. Hegarty, "Optimal and near-optimal detectors for acquisition of the GPS L5 signal," in *Proc. 2006 ION Nat. Tech. Meeting*, Monterey, CA, Jan. 2006, pp. 717–725.

[22] M. Pini, E. Viviani, L. Lo Presti, "GPS L5 signal acquisition exploiting Neumann-Hoffman code transitions," in *Proc. 2010 Int. ION Tech. Meeting*, San Diego, CA, Jan. 2010, pp. 765–772.

[23] D. Borio, "FFT sign search with secondary code constraints for GNSS signal acquisition," in *Proc. IEEE 68th Vehicular Technology. Conf.*, Calgary, AB, Canada, Sept. 2008, pp. 1–5.

[24] S.-H. Kong and B. Kim, "Ultra-fast L2-CL code acquisition for a dual band GPS receiver," *J. Pos. Navigat. Timing*, vol. 4, no. 4, pp. 151–160, 2015.

[25] C. Yang, "Joint acquisition of CM and CL codes for GPS L2 civil (L2C) signals," in *Proc. 61st Annu. Meeting ION*, Cambridge, MA, June 2005, pp. 553–562.

[26] M. L. Psiaki, "FFT-based acquisition of GPS L2 civilian CM and CL signals," in *Proc.* 17th *Int. Tech. Meeting ION GNSS*, Long Beach, CA, Sept. 2004, pp. 646–653.

[27] T. H. Ta, F. Dovis, D. Margaria, and L. L. Presti, "Comparative study on joint data/pilot strategies for high sensitivity Galileo E1 open service signal acquisition," *IET Radar Sonar Navigat.*, vol. 4, no. 6, pp. 764–779, 2010.

[28] D. Margaria, F. Dovis, and P. Mulassano, "Galileo AltBOC signal multiresolution acquisition strategy," *IEEE Aerosp. Electron. Syst. Mag.*, vol. 23, no. 11, pp. 4–10, 2008.

[29] C. Yang and A. Soloviev, "Joint acquisition of GNSS codes via coherent combining of multi-frequency composite quadrature signals," in *Proc. Int. Tech. Meeting ION*, Monterey, CA, Jan. 2016, pp. 805–819.

[30] C. Gernot, S. K. Shanmugam, K. O'keefe, and G. Lachapelle, "A novel L1 and L2C combined detection scheme for enhanced GPS acquisition," in *Proc.* 20th *Int. Tech. Meeting ION GNSS*, Fort Worth, TX, Sept. 2007, pp. 219–230.

[31] S.-H. Kong, "Fast multi-satellite ML acquisition for A-GPS," *IEEE Trans. Wireless Commun.*, vol. 13, no. 9, pp. 4935–4946, 2014.

[32] J. A. Starzyk and Z. Zhu, "Averaging correlation for C/A Code acquisition and tracking in frequency domain," in *Proc. 44th IEEE Midwest Symp. Circuits and Systems Conf.*, Aug. 2001, vol. 2, pp. 905–908.

[33] M. Sahmoudi, M. G. Amin, and R. Landry, Jr., "Acquisition of weak GNSS signals using a new block averaging pre-processing," in *Proc. IEEE/ION Position Location and Navigation Syst. Conf.*, May 2008, pp. 1362–1372.

[34] S.-H. Kong, "SDHT for fast detection of weak GNSS signals," *IEEE J. Sel. Areas Commun.*, vol. 33, no. 11, pp. 2366–2378, Nov. 2015.

[35] M. Monnerat, R. Couty, N. Vincent, O. Huez, and E. Chatre, "The assisted GNSS, technology and applications," in *Proc. Int. Tech. Meeting ION*, Long Beach, CA, Sept. 2004, pp. 2479–2488.

[36] N. Harper, *Server-Side GPS and Assisted-GPS in Java*. Norwood, MA: Artech House, 2009.

[37] 3GPP, "Position determination service standard for dual-mode spread spectrum systems," Telecommunication Industry Association, Rep. IS-801 TR45.5., Oct. 15, 1999.

[38] 3GPP, "Radio subsystem synchronization (Release 8)," 3GPP TS 45.010, May 2008.

[39] 3GPP, "User Equipment (UE) radio transmission and reception (FDD) (Release 8)," 3GPP TS 25.101., Sept. 2007.

[40] C. Fernandez-Prades, P. Closas, J. Vila'Valls, M. F. Naharro, and A. T. Sanjose, "Assisted GNSS in LTE-advanced networks and its application to vector tracking loops," in *Proc.* 25th *Int. Tech. Meeting ION*, Nashville, TN, Sept. 2012, pp. 1462–1476.

SP